Journal of
Applied Crystallography

ISSN 0021-8898

Received 28 August 2011
Accepted 22 September 2011

VESTA 3 for three-dimensional visualization of crystal, volumetric and morphology data

Koichi Momma*‡ and Fujio Izumi

Quantum Beam Unit, National Institute for Materials Science, 1-1 Namiki, Tsukuba, Ibaraki 305-0044, Japan. Correspondence e-mail: k-momma@kahaku.go.jp

VESTA is a three-dimensional visualization system for crystallographic studies and electronic state calculations. It has been upgraded to the latest version, *VESTA 3*, implementing new features including drawing the external morphology of crystals; superimposing multiple structural models, volumetric data and crystal faces; calculation of electron and nuclear densities from structure parameters; calculation of Patterson functions from structure parameters or volumetric data; integration of electron and nuclear densities by Voronoi tessellation; visualization of isosurfaces with multiple levels; determination of the best plane for selected atoms; an extended bond-search algorithm to enable more sophisticated searches in complex molecules and cage-like structures; undo and redo in graphical user interface operations; and significant performance improvements in rendering isosurfaces and calculating slices.

1. Introduction

VESTA is a program for three-dimensional visualization and investigation of crystal structures and volumetric (voxel) data, such as electron and coherent scattering length (nuclear) densities determined by X-ray and neutron diffraction, respectively. It also serves for visualization of volumetric data, including electron densities, wavefunctions and electrostatic potentials resulting from electronic state calculations. Thus, *VESTA* helps in the understanding of crystal structures and a variety of physical quantities in three dimensions.

VESTA originated from *VICS* and *VEND* in the *VENUS* software package (Izumi & Dilanian, 2005). *VICS* and *VEND* were developed for three-dimensional visualization of structural models and volumetric data, respectively, by making full use of OpenGL technology. Both of them were written in the C language with the graphical user interface (GUI) toolkits GLUT and GLUI, but these rapidly became obsolete owing to limited functionalities and the lack of upgrades.

To overcome this unfavourable situation, we first upgraded *VICS* to *VICS-II* by rewriting the core functionalities in C++ and constructing a new GUI framework utilizing the wxWidgets toolkit (Smart *et al.*, 2005). Next, *VICS-II* and *VEND* were integrated into a next-generation visualization system, *VESTA* (Momma & Izumi, 2006, 2008), the GUI of which is more user-friendly than that of *VICS* and *VEND*. Since its release, *VESTA* has been used extensively to contribute to several hundred papers in the fields of physics, chemistry, materials science (Izumi & Momma, 2008) and earth science (Momma & Izumi, 2010).

We have recently upgraded *VESTA* to the latest version, *VESTA 3*, to extend the range of its applications. This paper describes the main features that have been added to *VESTA* since the publication of our last paper (Momma & Izumi, 2008).

2. Overview

VESTA is capable of opening multiple files in a single instance of the program by use of a tab-based interface. Multiple windows can be created, each of which has multiple tab pages, as Fig. 1 illustrates.

Structural models are represented by ball-and-stick, space-filling, polyhedral, wireframe, stick and displacement ellipsoid models. On selection of atoms and bonds, a variety of crystallographic information is output to the text area below the graphic area. General equivalent positions in a standard lattice setting can be transformed into those in a nonstandard setting using a (4×4) transformation matrix (Arnold, 2005), which is also used to generate a superlattice and a sublattice.

Volumetric data, such as electron and nuclear densities, Patterson functions, and wavefunctions, are displayed as isosurfaces, bird's-eye views and two-dimensional maps containing contours. *VESTA* supports a feature of surface colouring to illustrate another kind of physical quantity at each point on the isosurfaces, typically isosurfaces of electron densities coloured in response to electrostatic potentials. Three kinds of electronic energy densities can be obtained from electron densities, according to procedures proposed by Tsirelson (2002). Laplacians of volumetric data can also be calculated for any type of data.

VESTA collaborates with external programs such as *STRUCTURE TIDY* (Gelato & Parthé, 1987), *RIETAN-FP* (Izumi & Momma, 2007), *ORFFE* (Busing *et al.*, 1964) and *MADEL* (Kato & Izumi, 2008). *STRUCTURE TIDY* allows the standardization of crystal structure data and the transformation of the current unit cell to a Niggli-reduced cell, as necessary. *RIETAN-FP* makes it possible to simulate X-ray and neutron powder diffraction patterns. The selection of four atoms in the graphic area gives information on fractional coordinates for imposing restraints on dihedral angles in Rietveld refinement with *RIETAN-FP*. The combination of *VESTA* and *ORFFE* provides a means for cross-checking geometric parameters by computer graphics. With *MADEL*, electrostatic site potentials and a Madelung energy are calculated from structure parameters by a Fourier method.

VESTA runs on three major operating systems, Microsoft Windows (XP/Vista/7), Mac OS X (10.5 or newer) and Linux.

3. New features

3.1. Crystal morphology

In addition to structural models and volumetric data, *VESTA* enables the display of crystal morphologies by inputting Miller

‡ Present address: National Museum of Nature and Science, 4-1-1, Amakubo, Tsukuba, Ibaraki, 305-0005, Japan.

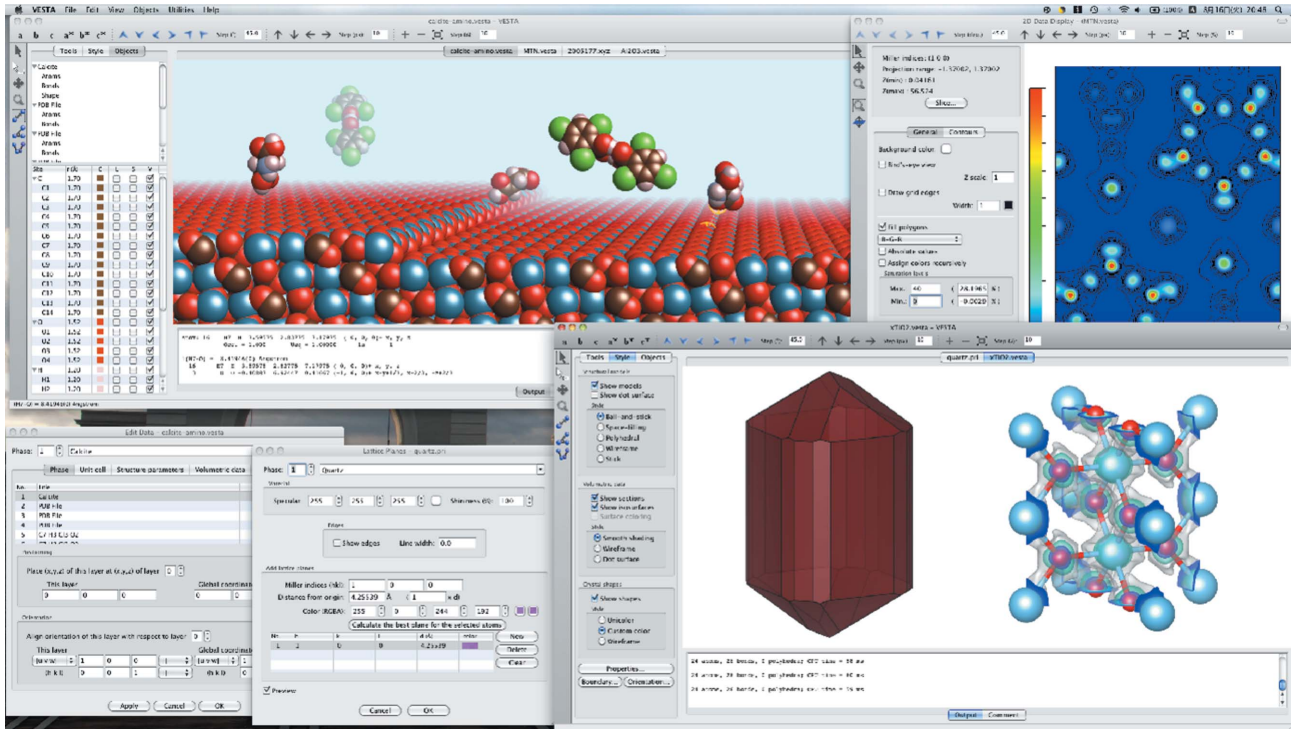

Figure 1
VESTA 3 running on Mac OS X.

indices. Crystal faces can be overlapped with both structural models and isosurfaces of volumetric data (Fig. 2*a*). Thus, the relationship between crystal morphologies and chemical bonds can be understood in three dimensions, for example by application of the periodic bond chain theory (Hartman, 1973). The morphologies of twinned crystals or of epitaxial intergrowths of two or more crystals are visualized by inputting multiple crystal data (Fig. 2*b*). After morphological data have been specified, information about the Miller indices, the distances from the centre of the crystal to the faces and the surface area of each face is output to the text area.

3.2. Overlaying multiple data

Two or more structures can be located in the same three-dimensional space to view them in the graphic area. For example, this feature greatly facilitates (*a*) the comparison of two structures; (*b*) the imaging of a chemical reaction or an interaction between two molecules; (*c*) the visualization of a variety of chemical species in layered or microporous materials; (*d*) the illustration of the adsorption of atoms and molecules onto the surface of a solid; and (*e*) the creation of interfaces between two structures (Fig. 3).

The relative positions and orientations of structures are specified by direct- and reciprocal-lattice vectors and the position of the origin

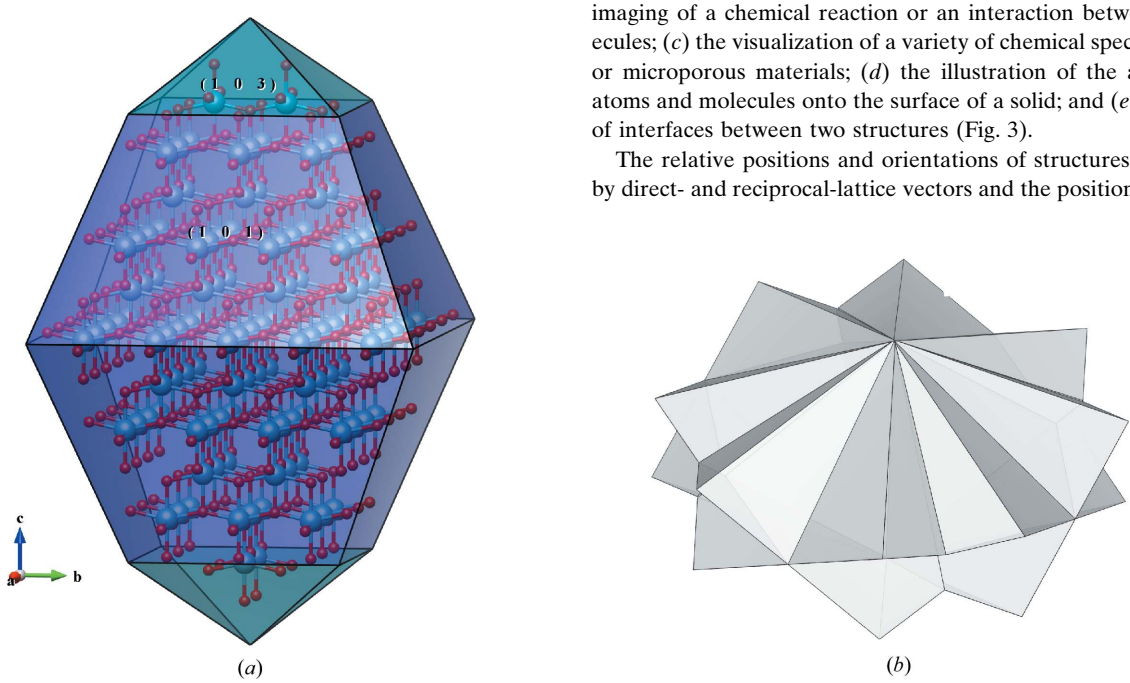

Figure 2
(*a*) Crystal morphology of anatase-type TiO_2 superimposed on its structural model. (*b*) A repeated twin of potassic feldspar composed of eight individuals according to the Babeno and Manebach laws.

for each structure. Not only structural models but also multiple sets of volumetric data and crystal morphologies can be overlaid with each other.

3.3. Model electron and nuclear densities

Model electron densities are obtained by the Fourier transform of structure factors calculated from structure parameters and atomic scattering factors, f_0, of neutral atoms (Waasmaier & Kirfel, 1995). The spatial resolution of electron densities is specified in units of ångström. Values of f_0 calculated from 11 coefficients compiled by Waasmaier & Kirfel (1995) are only reliable enough in the range of $(\sin\theta)/\lambda < 6$ Å^{-1}, which corresponds to a spatial resolution of *ca* 0.042 Å. *VESTA* simply extrapolates the f_0 values even when the specified resolution is smaller than 0.042 Å. The number of grids along each crystallographic axis, N_x, is automatically set such that N_x gives a resolution close to the specified value and N_x satisfies symmetrical constraints. Fig. 4 illustrates the model electron densities in azurite, $Cu_3(CO_3)_2(OH)_2$. Model nuclear densities are calculated in the same manner from structure parameters and bound coherent scattering lengths, b_c, of the elements (Sears, 2004).

This feature is used, for instance, to visualize differences between electron densities determined experimentally by the maximum entropy method (MEM) (Collins, 1982; Sakata *et al.*, 1992) or MEM-based pattern fitting (Izumi & Dilanian, 2002; Izumi, 2004) and those simulated in the way described above.

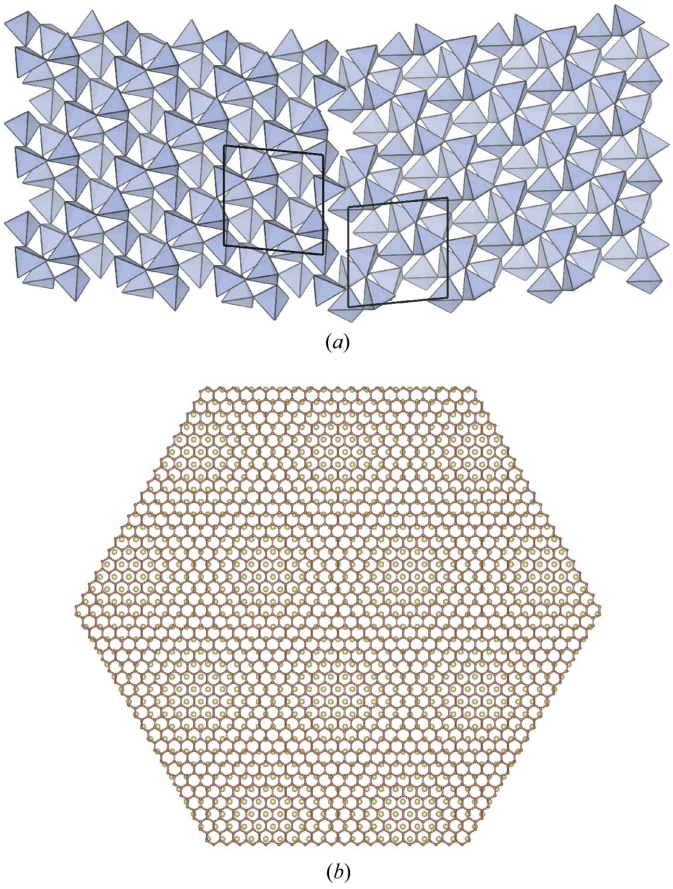

Figure 3
(*a*) An unrelaxed twin-boundary structure of the type-I Japan twin of quartz (Momma *et al.*, 2009). The black rectangles show the unit cells corresponding to the twin lattice. (*b*) A *moiré* pattern generated by graphene on the (111) surface of iridium.

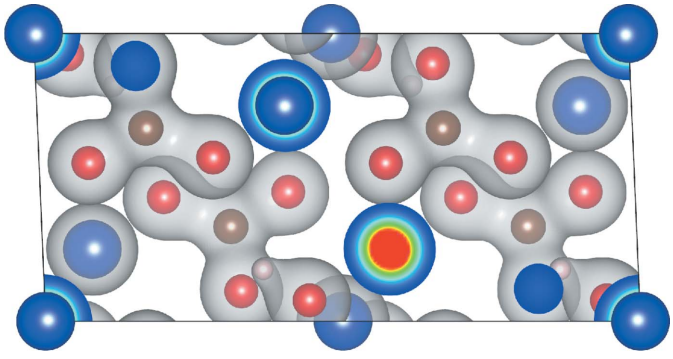

Figure 4
Model electron densities of azurite, drawn with an isosurface level of 1 Å^{-3}.

Table 1
Results of peak search and Voronoi tesselation for electron densities in NaV_6O_{11}.

Site	Peak density (Å^{-1})	Number of electrons	Voronoi volume (Å^3)
V1	802	21.3	7.6
V2	884	21.4	7.7
V3	855	21.3	8.6
O1	74	8.9	11.1
O2	74	8.9	11.2
O3	74	9.0	11.0
Na	45	10.8	15.5

3.4. Patterson functions

Patterson functions in the unit cell are calculated in three different ways: (*a*) from structure parameters and values of f_0 (Waasmaier & Kirfel, 1995); (*b*) from structure parameters and values of b_c (Sears, 2004); and (*c*) by convolution of volumetric data that are currently displayed in the graphic area. In the first and second cases, the spatial resolution of the Patterson function is input by users in units of ångström, and in the third case the resolution is the same as that of the volumetric data.

3.5. Local integration of volumetric data

During searches for peaks in volumetric data, *VESTA* calculates the values of the integral and Voronoi volumes for the peaks found in the unit cell, on the basis of Voronoi tessellation (Press *et al.*, 2007). The integration of electron densities resulting from MEM analysis gives the number of electrons around each crystallographic site, enabling us to extract information on the oxidation states of the atoms and charge transfer between atoms bonded to each other.

Table 1 lists the results of a peak search for electron densities in the unit cell of NaV_6O_{11} (Kanke *et al.*, 1992). Each value of the integral, which corresponds to the number of electrons per site, was calculated by summing the electron densities, as determined by MEM-based pattern fitting (Izumi & Dilanian, 2002; Izumi, 2004) from synchrotron X-ray powder diffraction data measured at a wavelength of 0.6358 Å.

3.6. Multiple levels of isosurfaces

While only one level of isosurfaces was visible at any one time in previous versions of *VESTA*, isosurfaces with any number of levels can now be drawn (Fig. 5). Because each isosurface only expresses a section of a certain level, the superimposition of multiple isosurfaces helps in the more intuitive understanding of the spatial distribution of volumetric data.

3.7. The best plane for selected atoms

The least-squares mean plane for a set of atoms selected by the user can be determined and displayed in the graphic area. This feature is used, firstly, through the 'lattice planes' dialogue box for the insertion of lattice planes into the graphic area and, secondly, in the 'two-dimensional data display' window for drawing a two-dimensional slice as a coloured contour map or a bird's-eye view.

3.8. Information on atoms

VESTA internally derives multiplicities, Wyckoff letters and site symmetries to display them after structural data have been read in or after an atom has been selected in the graphic area.

The selection of atoms in a displacement ellipsoid model affords the principal axes and mean-square displacements in the text area (Fig. 6*a*). If one or more of the principal axes have a negative mean-square displacement, the atoms are represented by cuboids so that the unusual atomic displacement parameters can be easily recognized (Fig. 6*b*). The cuboid is oriented in accordance with the principal axes, with the dimensions of the cuboid scaled according to the absolute value of the mean-square displacement along each principal axis.

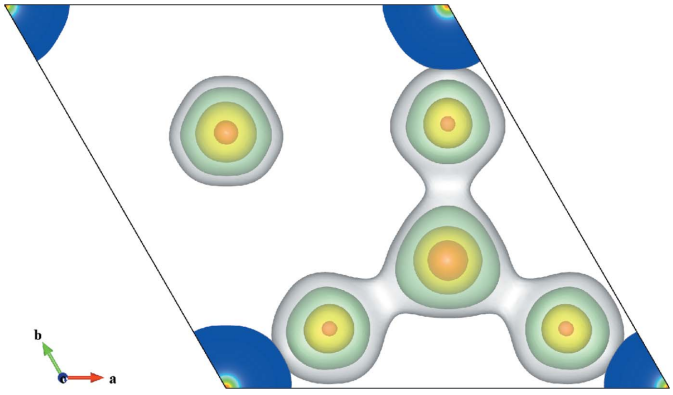

Figure 5
Electron-density distributions in NaV_6O_{11}, determined by MEM-based pattern fitting from synchrotron X-ray powder diffraction data (Kanke *et al.*, 1992). Isosurface levels are at 1, 2.5, 8 and 40 Å^{-3}.

```
Atom:  2    O1  O  0.790/0  0.58138  0.50000  ( 1, 1, 0)+ -x+y, -x, z+1/3
            Occ. = 1.000       Ueq = 0.05605      6j      ..2

Principal axes of the anisotropic atomic displacement parameters
       MSD (Å^2)      x          y          z          u          v          w
  1     0.095/93    -0.210944 -0.033032  0.224063    -0.046052 -0.00/636  0.041084
  2     0.054966     0.004491  0.231251  0.038319     0.02/630  0.053462  0.00/026
  3     0.01/392     0.0964/1 -0.016519  0.088388     0.01/405 -0.003819  0.01620/
```

(*a*)

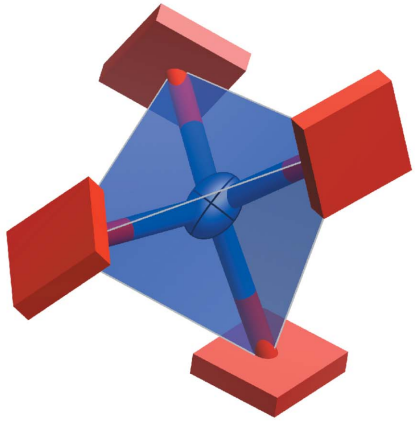

(*b*)

Figure 6
(*a*) Information on the anisotropic atomic displacement of a selected atom. Columns `x`, `y` and `z` denote the principal axes represented in the Cartesian coordinate system, and columns `u`, `v` and `w` are those represented in fractional coordinates. (*b*) A displacement ellipsoid model of a structure, with some atoms having negative mean-square displacements.

3.9. Enhancement in bond-search algorithm

A sophisticated bond-search algorithm is adopted in *VESTA* lest coordination polyhedra or molecules be truncated. The algorithm is extended to better suit complex molecules and microporous materials. Even if some of the bond lengths in the molecules are greater than the intermolecular distances, all atoms in the molecules are searched thoroughly. Framework atoms and bonds in cage-like structures can also be searched and displayed more readily, as Fig. 7 shows.

3.10. Customization of symmetry operations

In addition to the transformation of symmetry operations by a (4×4) matrix, symmetry operations may also be edited manually. In that case, the symmetry operations do not necessarily form a closed group. This feature can be used, for example, when a structure has pseudosymmetry that cannot be represented by any of the conventional space groups.

3.11. Undo and redo

The actions of the user can now be undone and redone. Only a very small amount of memory is used for this history information. The number of undo and redo operations is virtually unlimited, provided the memory capacity is sufficient.

3.12. General improvements in image displays and GUI

The rendering of isosurfaces has been greatly accelerated. The speed of calculating two-dimensional sections in volumetric data has also been increased by a factor of more than ten. If more than one element occupies the same crystallographic site, or if the occupancy of a site is less than unity, the atom is displayed as a circle graph representing the occupancies of the constituent elements. The labels of the atoms can be displayed near them, and more than two vectors (arrows) can be attached to each atom.

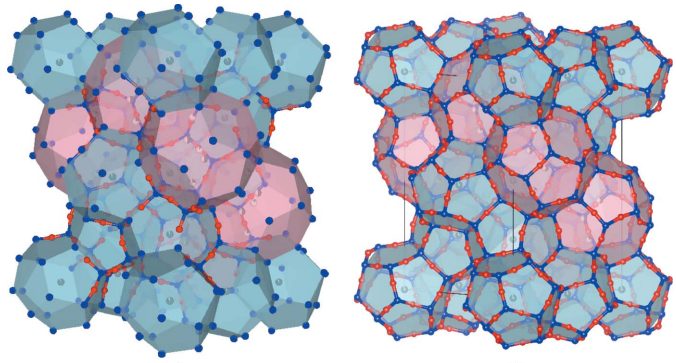

(*a*) (*b*)

Figure 7
The crystal structure of chibaite, a natural analogue of the MTN-type silica clathrate compound (Momma *et al.*, 2011), drawn with (*a*) *VESTA 2.x* and (*b*) *VESTA 3*. With *VESTA 3*, all the oxygen atoms at the edges of the cages are automatically searched and drawn.

The properties (colour, size, resolution *etc.*) of atoms, bonds and polyhedra can be set more flexibly from a list of objects in the left-hand panel of the main window.

3.13. Improved support for various file formats

VESTA is able to read in files in 42 types of format, which includes 28 formats for structural models, nine for volumetric data, and five for both structural and volumetric data. File formats newly supported are *GSAS* `*.exp` files (Larson & Von Dreele, 2004), *SHELX* `*.ins` files (Sheldrick, 2008), files output by *STRUCTURE TIDY* (`*.sto`) (Gelato & Parthé, 1987), and structure and charge-density data output by *CASTEP* (`*.cell` and `*.charg_frm`) (Segall *et al.*, 2002; Clark *et al.*, 2002). For output files, 16 formats are supported, of which two are new: the *PRIMA* volumetric data format (`*.pri`) (Izumi & Dilanian, 2002) and the *VASP* POSCAR format (Kresse & Furthmüller, 1996).

Space-group symmetry and the choice of origin can be read in from a CIF (crystallographic information file; Hall *et al.*, 1991), even when neither a Hermann–Mauguin symbol nor a space-group number is recorded in the file, as long as the symmetry operations are recorded. Files in the Protein Data Bank (`*.pdb`) format (Berman *et al.*, 2003) and the *XCrySDen* `*.xsf` format (Kokalj, 2003) can now be input more reliably.

4. Distribution and documentation

Executable binary files of *VESTA 3* are available free of charge from http://www.geocities.jp/kmo_mma/. For Windows and Linux, both 32- and 64-bit applications are provided, while only a 64-bit version is distributed for Mac OS X. Full details of *VESTA* and its licence agreement are documented in the user manual, which can also be downloaded from the above web site. For users of older computers, and for compatibility with files created by the older versions of *VESTA*, distribution of the *VESTA 2.x* series will be continued in parallel with that of *VESTA 3*.

Takashi Ida of Nagoya Institute of Technology is acknowledged for kindly providing us with the initial code for Voronoi tessellation.

References

Arnold, H. (2005). *International Tables for Crystallography*, Vol. A, 5th ed., edited by Th. Hahn, pp. 78–85. Heidelberg: Springer.

Berman, H., Henrick, K. & Nakamura, H. (2003). *Nat. Struct. Biol.* **10**, 980.

Busing, W. R., Martin, K. O. & Levy, H. A. (1964). *A FORTRAN Crystallographic Function and Error Program.* Report ORNL-TM-306, Oak Ridge National Laboratory, Tennessee, USA.

Clark, S. J., Segall, M. D., Pickard, C. J., Hasnip, P. J., Probert, M. J., Refson, K. & Payne, M. C. (2002). *Z. Kristallogr.* **220**, 567–570.

Collins, D. M. (1982). *Nature* (*London*), **298**, 49–51.

Gelato, L. M. & Parthé, E. (1987). *J. Appl. Cryst.* **20**, 139–143.

Hall, S. R., Allen, F. H. & Brown, I. D. (1991). *Acta Cryst.* A**47**, 655–685.

Hartman, P. (1973). *Crystal Growth: An Introduction*, pp. 398–401. Amsterdam: North-Holland Publishing Co.

Izumi, F. (2004). *Solid State Ionics*, **172**, 1–6.

Izumi, F. & Dilanian, R. A. (2002). *Recent Research Developments in Physics*, Vol. 3, part II, pp. 699–726. Trivandrum: Transworld Research Network.

Izumi, F. & Dilanian, R. A. (2005). *IUCr Commission on Powder Diffraction Newsletter*, No. 32, pp. 59–63.

Izumi, F. & Momma, K. (2007). *Solid State Phenom.* **130**, 15–20.

Izumi, F. & Momma, K. (2008). *Bull. Ceram. Soc. Jpn*, **43**, 902–908.

Kanke, Y., Kato, K., Takayama-Muromachi, E. & Isobe, M. (1992). *Acta Cryst.* C**48**, 1376–1380.

Kato, K. & Izumi, F. (2008). Unpublished work.

Kokalj, A. (2003). *Comput. Mater. Sci.* **28**, 155–168.

Kresse, G. & Furthmüller, J. (1996). *Phys. Rev. B*, **54**, 11169–11186.

Larson, A. C. & Von Dreele, R. B. (2004). *GSAS*. Report LAUR 86-748. Los Alamos National Laboratory, New Mexico, USA.

Momma, K., Ikeda, T., Nishikubo, K., Takahashi, N., Honma, C., Takada, M., Furukawa, Y., Nagase, T. & Kudoh, Y. (2011). *Nat. Commun.* **2**, 196.

Momma, K. & Izumi, F. (2006). *IUCr Commission on Crystallographic Computing Newsletter*, No. 7, pp. 106–119.

Momma, K. & Izumi, F. (2008). *J. Appl. Cryst.* **41**, 653–658.

Momma, K. & Izumi, F. (2010). *Jpn. Mag. Mineral. Petrol. Sci.* **39**, 136–145.

Momma, K., Nagase, T., Kuribayashi, T. & Kudoh, Y. (2009). *Eur. J. Mineral.* **21**, 373–383.

Press, W. H., Flannery, B. P., Teukolsky, S. A. & Vetterling, W. T. (2007). *Numerical Recipes: The Art of Scientific Computing*, 3rd ed., pp. 1142–1146. New York: Cambridge University Press.

Sakata, M., Uno, T., Takata, M. & Mori, R. (1992). *Acta Cryst.* B**48**, 591–598.

Sears, V. F. (2004). *International Tables for Crystallography*, Vol. C, 3rd ed., edited by E. Prince, pp. 444–452. Dordrecht: Kluwer.

Segall, M. D., Lindan, P. J. D., Probert, M. J., Pickard, C. J., Hasnip, P. J., Clark, S. J. & Payne, M. C. (2002). *J. Phys. Condens. Matter*, **14**, 2717–2743.

Sheldrick, G. M. (2008). *Acta Cryst.* A**64**, 112–122.

Smart, J., Hock, K. & Csomor, S. (2005). *Cross-Platform GUI Programming with wxWidgets.* Upper Saddle River: Prentice Hall.

Tsirelson, V. G. (2002). *Acta Cryst.* B**58**, 632–639.

Waasmaier, D. & Kirfel, A. (1995). *Acta Cryst.* A**51**, 416–431.